



Structural and biochemical analyses of *Microcystis aeruginosa* O-acetylserine sulfhydrylases reveal a negative feedback regulation of cysteine biosynthesis

Mo Lu¹, Bo-Ying Xu¹, Kang Zhou, Wang Cheng, Yong-Liang Jiang, Yuxing Chen, Cong-Zhao Zhou*

Hefei National Laboratory for Physical Sciences at the Microscale and School of Life Sciences, University of Science and Technology of China, Hefei, Anhui 230027, People's Republic of China

ARTICLE INFO

Article history:

Received 16 September 2013

Received in revised form 15 November 2013

Accepted 15 November 2013

Available online 23 November 2013

Keywords:

Cyanobacteria

Crystal structure

O-acetylserine sulfhydrylase

Enzymatic activity

Redox

ABSTRACT

O-acetylserine sulfhydrylase (OASS) catalyzes the final step of cysteine biosynthesis from O-acetylserine (OAS) and inorganic sulfide in plants and bacteria. Bioinformatics analyses combined with activity assays enabled us to annotate the two putative genes of *Microcystis aeruginosa* PCC 7806 to CysK1 and CysK2, which encode the two 75% sequence-identical OASS paralogs. Moreover, we solved the crystal structures of CysK1 at 2.30 Å and cystine-complexed CysK2 at 1.91 Å, revealing a quite similar overall structure that belongs to the family of fold-type II PLP-dependent enzymes. Structural comparison indicated a significant induced fit upon binding to the cystine, which occupies the binding site for the substrate OAS and blocks the product release tunnel. Subsequent enzymatic assays further confirmed that cystine is a competitive inhibitor of the substrate OAS. Moreover, multiple-sequence alignment revealed that the cystine-binding residues are highly conserved in all OASS proteins, suggesting that this auto-inhibition of cystine might be a universal mechanism of cysteine biosynthesis pathway.

© 2013 Elsevier B.V. All rights reserved.

1. Introduction

In plants and bacteria, the de novo biosynthesis of L-cysteine involves two enzymes: serine acetyl transferase (SAT, EC 2.3.1.30) and O-acetylserine sulfhydrylase (OASS, EC 2.5.1.47) (Scheme 1). SAT catalyzes the production of O-acetylserine (OAS) by transferring the acetyl group from acetyl coenzyme A to serine. Afterwards, OASS catalyzes the formation of cysteine from OAS and sulfide using pyridoxal 5'-phosphate (PLP) as a cofactor [1,2]. The catalysis of OASS follows a ping-pong mechanism that is typical for PLP-dependent enzymes [3]. In detail, the reaction can be divided into two halves. The cofactor in the resting-state enzyme forms an internal Schiff base with the invariant catalytic lysine residue. The incoming substrate then forms an external Schiff base with PLP, followed by a β-elimination reaction in which acetate is released and a proton is abstracted from the α-position, most likely by the side chain of lysine [4]. At the end of the first half reaction, an α-aminoacrylate intermediate is covalently linked to PLP [5]. The second half reaction starts with a nucleophilic attack of the sulfide (or HS⁻) on the β-carbon of the aminoacrylate intermediate and the α-carbon is re-protonated, resulting in an external Schiff base

bound cysteine, which is finally released accompanied with the regeneration of an internal aldimine [6,7].

The cysteine biosynthesis and sulfur homeostasis are finely regulated by a feedback circuit. In plants and bacteria, SAT and CysK form a hetero-oligomeric cysteine synthase complex at the high sulfur level, leaving CysK inactivated [8,9]. Upon the decrease of sulfur concentration, CysK is dissociated from the complex and activated to produce cysteine, which in turn could be fed back to inhibit the activity of SAT [10] (Scheme 1).

Most bacteria encode two types of 25–45% sequence-identical OASSs, denoted as CysK and CysM, respectively [11]. The constitutively expressed CysK, which is a major enzyme, has been well characterized [12–18]. In contrast, CysM contributes up to only about 20% of the total cysteine biosynthesis activity [11,19]. Distinguishing from CysK that solely uses H₂S as the sulfur donor, CysM can use H₂S or larger substrates such as thiosulfate [20]. This difference of substrate specificity is determined by a flexible loop located at the entrance of active-site pocket [21]. CysK is featured by a short loop containing small residues “GAG” (G230, A231 and G232 in the case of *Salmonella typhimurium* CysK). In contrast, CysM has a much longer loop containing larger residues (R210, R211 and W212 in the case of *Escherichia coli* CysM), in addition to an insertion of three residues. However, both CysK and CysM share a highly conserved OAS-binding site. Moreover, the OASSs of known structure share an overall structure that belongs to the fold-type II class [22–30].

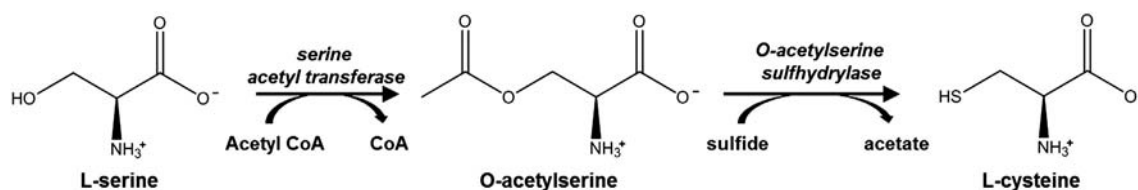
The cyanobacterium *Microcystis aeruginosa* PCC 7806 encodes three putative OASSs: CA086616, CA086589 and CA086970. Sequence

Abbreviations: SAT, serine acetyl transferase; OASS, O-acetylserine sulfhydrylase; OAS, O-acetylserine; PLP, pyridoxal 5'-phosphate; RMSD, root-mean square deviation; GSSG, glutathione disulfide; DTT, dithiothreitol; MOPS, 4-morpholinethanesulfonic acid

* Corresponding author at: Tel./fax: +86 551 63600406.

E-mail address: zc@ustc.edu.cn (C.-Z. Zhou).

¹ Both authors contributed equally to this work.



Scheme 1. Schematic representation of the cysteine biosynthesis pathway.

comparison indicated that CA086616 and CA086589 share a sequence identity of 75% to each other, and 40–66% to CysK proteins of known structure [23–30]. Moreover, they both have a highly conserved “GAG” motif, thus termed CysK1 and CysK2, respectively. Here we solved the crystal structures of CysK1 and cystine-complexed CysK2 (termed CysK2–cystine) at 2.30 and 1.91 Å resolution, respectively. Structural analysis in combination with enzymatic assays enabled us to definitely annotate *M. aeruginosa* CA086616 and CA086589 to CysK1 and CysK2, respectively. Furthermore, we found that CysK could be auto-inhibited by the oxidized product, suggesting a putative mechanism of negative feedback regulation of cysteine biosynthesis.

2. Materials and methods

2.1. Cloning, expression and purification of CysK1 and CysK2

The coding sequences of CysK1/CA086616 and CysK2/CA086589 were amplified from the genomic DNA of *M. aeruginosa* PCC 7806 by PCR, respectively. The PCR products were cloned into a pET28a-derived expression vector with a hexahistidine tag added to the N-terminus of the recombinant proteins, and transformed into *E. coli* strain BL21 (DE3) (Novagen) using 2 × YT culture medium (5 g of NaCl, 16 g of Bacto-Tryptone, and 10 g of yeast extract per liter). The transformed cells were grown at 37 °C in 2 × YT medium containing 30 µg/ml kanamycin until the OD_{600nm} reached about 0.6–0.8. Expression of the recombinant proteins was then induced with 0.2 mM isopropyl β-D-1-thiogalactopyranoside for another 20 h at 16 °C before harvesting. Cells were collected by centrifugation at 4000 ×g for 20 min and resuspended in 40 ml lysis buffer (20 mM Tris–HCl, pH 8.0, and 200 mM NaCl). After 10 min of sonication and centrifugation at 12,000 ×g for 30 min, the supernatant containing the target protein was collected and loaded onto a Ni-NTA column (GE healthcare) equilibrated with the binding buffer (20 mM Tris–HCl, pH 8.0, and 200 mM NaCl). The target protein was eluted with 300 mM imidazole, and further loaded onto a Superdex 200 column (GE Healthcare; 20 mM Tris–HCl, pH 7.0, 150 mM NaCl, 14 mM β-mercaptoethanol). Fractions containing the target protein were pooled and concentrated to 10 mg/ml by ultrafiltration (Millipore Corp., Amicon) for crystallization trials. The purity of protein was assessed by sodium dodecyl sulfate polyacrylamide gel electrophoresis (SDS-PAGE) and the protein sample was flash-frozen in liquid nitrogen and stored at –80 °C.

2.2. Crystallization, data collection and processing

Crystals of CysK1 and CysK2 were grown at 16 °C using the hanging drop vapor-diffusion techniques. After extensive screening and optimization, two conditions were established that resulted in single crystals of CysK1 and CysK2. Crystals of CysK1 were obtained by mixing the protein sample (10 mg/ml) with an equal volume of the reservoir solution [0.1 M 4-morpholineethanesulfonic acid (MOPS), pH 6.0, 60% 2-methyl-2,4-pentanediol]. Crystals of CysK2 were obtained by mixing the protein sample at 10 mg/ml with an equal volume of the reservoir solution [1.5 M (NH₄)₂SO₄, 0.1 M Bis–Tris–propane, pH 7.0]. Co-crystallization trials of CysK1 or CysK2 with cysteine were performed

using the crystallization conditions established for the corresponding enzyme after mixing with cysteine at a final concentration of 10 mM.

Crystals of the two proteins were transferred to cryoprotectant (reservoir solution supplemented with 30% glycerol) and flash-cooled with liquid nitrogen. All diffraction data were collected at 100 K in a liquid nitrogen stream using beamline 17U with an MX-225 CCD detector (Marresearch GmbH, Norderstedt, Germany) at the Shanghai Synchrotron Radiation Facility. All diffraction data were integrated and scaled with the program HKL2000 [31].

2.3. Structure determination and refinement

The crystal structures of CysK1 and CysK2 were determined by molecular replacement with MOLREP [32] using the coordinates of *Mycobacterium tuberculosis* OASS (PDB ID: 2Q3B) as the search model, respectively. Electron density maps showed clear features of secondary-structure elements. The initial model was refined using the maximum likelihood method implemented in REFMAC5 [33] as part of CCP4i program suite [34] and rebuild interactively using the unbiased electron density maps with coefficients $F_o - F_c$ in the program COOT [35]. The final model was evaluated with the programs MOLPROBITY [36] and PROCHECK [37]. Crystallographic parameters were listed in Table 1. All structure figures were prepared with the program PyMOL [38].

2.4. Substrate/product binding constants

The chemicals OAS, cysteine and cystine were bought from Sangon, China. According to the previous procedure [25], binding affinities of CysK1 and CysK2 towards OAS, cysteine and cystine were measured by monitoring the change of PLP, using a DU800 UV/visible spectrophotometer (Beckman Coulter, Fullerton, CA, USA). Titrations of OAS (0–1.2 mM), cysteine (0–2.0 mM) and cystine (0–1.0 mM) against 30 µM CysK1 or CysK2 were performed at 25 °C in the buffer of 0.1 M Tris–HCl, pH 7.0. Dissociation constant (K_d) was calculated by fitting the data to a reversible two-state binding model, $\Delta A = (\Delta A_{\max}[L]) / (K_d + [L])$, using the program Origin 7.5, where ΔA is the change in absorbance at a given wavelength in the presence of OAS/cysteine/cystine at concentration [L]. The assays were performed three times, and expressed as a mean ± standard error (S.E.).

2.5. Enzymatic activity and inhibition assays

The OASS activity of the recombinant CysK1 or CysK2 was assayed with spectrophotometry by monitoring the absorbance at 559 nm upon the formation of cysteine using the acid–ninhydrin method [39]. Standard reactions were carried out in 250 µl of 100 mM MOPS, pH 7.0, 10 mM OAS and 0.25 mM sodium sulfide. The reactions were started by the addition of the enzyme to 200 nM and incubated for 0.5, 5, and 10 min at 25 °C. The addition of trichloroacetic acid to a final concentration of 16.6% stopped the reactions. Following centrifugation, the amount of product was determined spectrophotometrically using a standard curve for cysteine in the range of 0.01–1.0 mM. According to the previous procedure [40], the reactions were performed to detect the effect of redox on CysK1/CysK2, added with 1 mM dithiothreitol (DTT) to mimic the physiological condition and 1 mM

Table 1
Crystal parameters, data collection and structure refinement statistics.

	CysK1 ^a	CysK2–cystine ^a
<i>Data collection</i>		
Space group	P2 ₁ 2 ₁ 2 ₁	P6 ₃ 22
Unit cell		
<i>a</i> , <i>b</i> , <i>c</i> (Å)	56.56, 93.83, 125.31	99.85, 99.85, 164.14
α, β, γ (°)	90.00	90.00, 90.00, 120.00
Resolution range (Å)	50.00–2.30 (2.38–2.30)	50.00–1.91 (1.98–1.91)
Unique reflections	29,900 (2943)	38,074 (3686)
Completeness (%)	99.1 (99.3)	99.6 (98.5)
<I/σ(I)>	16.6 (5.0)	36.0 (8.4)
R _{merge} ^b (%)	9.9 (43.0)	7.6 (43.6)
Average redundancy	6.0 (6.1)	20.9 (20.0)
<i>Structure refinement</i>		
Resolution range (Å)	46.92–2.30	32.06–1.91
R-factor ^c /R-free ^d (%)	18.3/22.3	20.2/23.0
Number of protein atoms	4742	2335
Number of water atoms	197	220
RMSD ^e bond lengths (Å)	0.006	0.009
RMSD bond angles (°)	1.090	1.304
Mean B factors (Å ²)	33.82	33.20
Average B factors ligand atoms ((Å ²))		39.0
<i>Ramachandran plot^f</i>		
(residues, %)		
Most favored (%)	97.44	97.08
Additional allowed (%)	2.56	2.92
Outliers (%)	0	0
PDB ID	4LMA	4LMB

^a The values in parentheses refer to statistics in the highest bin.

^b $R_{\text{merge}} = \frac{\sum_{\text{hkl}} \sum_i |I_i(\text{hkl}) - \langle I(\text{hkl}) \rangle|}{\sum_{\text{hkl}} \sum_i I_i(\text{hkl})}$, where $I_i(\text{hkl})$ is the intensity of an observation and $\langle I(\text{hkl}) \rangle$ is the mean value for its unique reflection; summations are over all reflections.

^c $R\text{-factor} = \frac{\sum_h |F_o(h) - F_c(h)|}{\sum_h F_o(h)}$, where F_o and F_c are the observed and calculated structure-factor amplitudes, respectively.

^d R-free was calculated with 5% of the data excluded from the refinement.

^e Root-mean square-deviation from ideal values.

^f Categories were defined by Molprobit.

glutathione disulfide (GSSG) to mimic the oxidative condition. The total amount of cysteine produced in the reaction with GSSG was recorded by adding 1 mM DTT to the products. The amount of synthesized cysteine was recorded as a function of time (0–60 min). Steady state kinetic parameters were determined by initial velocity experiments, using the above assay with varying OAS concentrations in the range 0–10.0 mM with a constant sodium sulfide concentration of 1.0 mM. Each measurement was carried out in triplicate. Michaelis–Menten parameters (V_{max} and K_m) were extracted from these data by nonlinear fitting to the Michaelis–Menten equation, $v = (V_{\text{max}}[S]) / (K_m + [S])$, using the program Origin 7.5.

The inhibition assays were performed in the buffer consisting of 100 mM MOPS buffer, pH 7.0. CysK1 or CysK2 at a concentration of 500 nM in a total volume of 250 μl was mixed with cystine at concentrations of 10, 100, 200, 400 and 800 μM. The wavelength at 559 nm was recorded using a DU800 spectrophotometer (Beckman Coulter, Fullerton, CA, USA). The initial rate of cysteine formation at 25 °C was determined in the absence or presence of various cystine concentrations, and varying OAS concentrations in the range 1.0–10.0 mM with a constant sodium sulfide concentration of 1.0 mM. At various time intervals, aliquots of the reaction mixture were removed and assayed for L-cysteine formation as described above. K_i is the dissociation constant of the enzyme towards the inhibitor. Substrate–velocity curves are generated in the presence of various concentrations of inhibitor. The mode of inhibition was determined from nonlinear regression and global curve fitting [41]. The rate equation is $v = (V_{\text{max}}[S]) / (K_m(1 + [I] / K_i) + [S])$. The assays were performed three times, and expressed as a mean ± S.E. for $n = 3$.

3. Results and discussion

3.1. Annotation and activity assays of *M. aeruginosa* CA086616/CysK1 and CA086589/CysK2

To annotate the two putative *M. aeruginosa* OASSs: CA086616 and CA086589, we searched the deduced protein sequences against the non-redundant protein sequence database using the BLAST program (www.ncbi.nlm.nih.gov/BLAST). CysK1 and CysK2 share a sequence identity of 75% to each other, and 40–66% to the previously identified CysK proteins (Fig. 1). Moreover, they possess a highly conserved catalytic lysine and a motif of “GAG” (Fig. 1, labeled with a black triangle and red asterisks respectively), which is featured by CysK proteins in bacteria and plants. Thus CA086616 and CA086589 are termed CysK1 and CysK2, respectively.

To further confirm our annotations, we purified the recombinant CysK1 and CysK2 for the activity assays. The purified proteins were in yellow with a maximum absorbance at 408 nm, indicating the presence of cofactor PLP [42]. Afterwards, specific activities of CysK1 and CysK2 towards the substrates OAS and sodium sulfide were determined by monitoring the formation of cysteine, as previously described [39]. CysK1 and CysK2 have an optimal reaction temperature of 25 °C and a turnover number of 132 and 232 s⁻¹, respectively, which are comparable to that (211 s⁻¹ at 30 °C) of the counterpart enzyme from *M. tuberculosis* [26]. The specific activities of the two enzymes are 235 and 412 μmol min⁻¹ mg⁻¹ protein, respectively. These results demonstrated that the two *M. aeruginosa* proteins CA086616 and CA086589 indeed encode two active OASSs.

3.2. Overall structures of CysK1 and CysK2

To further investigate the structural features of these cyanobacterial OASSs, we determined structures of CysK1 and CysK2–cystine at 2.30 Å and 1.91 Å resolution by molecular replacement, respectively (Fig. 2A and 2B). For both structures, each asymmetric unit contains one molecule, and the symmetric operation enables us to define a homodimer with 2-fold crystallographic axis (Fig. 2A and B). The total buried dimeric interface is 2280 Å² for CysK1 and 1984 Å² for CysK2. Both CysK1 and CysK2 exist as a dimer in solution, as proven by gel-filtration chromatography and native gel electrophoresis.

In both CysK1 and CysK2–cystine structures, each subunit consists of two α/β domains, similar to the typical fold-type II PLP enzymes (Fig. 2A and B). The N-terminal domain is composed of a central four-stranded parallel β-sheet (β3–β6) surrounded by four α-helices (α2–α5), and the C-terminal domain comprises a six-stranded mixed β-sheet (β1–β2, β7–β10) sandwiched by five α-helices (α6–α10). The dimeric interface is formed by three α-helices (α4, α7 and α9) and three loops from each subunit and stabilized primarily by hydrogen bonds and salt bridges. A structural similarity search using Dali program (http://ekhidna.biocenter.helsinki.fi/dali_server/) produced a list of outputs including the top five OASSs from *M. tuberculosis* [26], *Glycine max* [28], *S. typhimurium* [24], *Entamoeba histolytica* [27], and *Arabidopsis thaliana* [25]. Structural superposition of CysK2 against these homologs gave a root-mean square deviation (RMSD) of 0.45 to 0.84 Å over 226–268 Cα atoms.

The overall structures of CysK1 and CysK2 are quite similar to each other with an RMSD of 0.42 Å over 225 Cα atoms, which enable us to superimpose the structure CysK1 against that of CysK2–cystine to observe the conformational changes upon cystine binding. Despite the C-terminal domains could be well superimposed, the N-terminal domain undergoes a significant induced fit upon cystine binding (Fig. 2C). The main chains of the conserved sequence stretch T⁷⁴SGNT⁷⁸, in addition to two loops (β4–α4, residues Met97–Glu104; and β5–α5, residues Pro120–Gly127) at the entrance of the catalytic pocket, shift approximately 5 Å towards the active site (Fig. 2C). All these

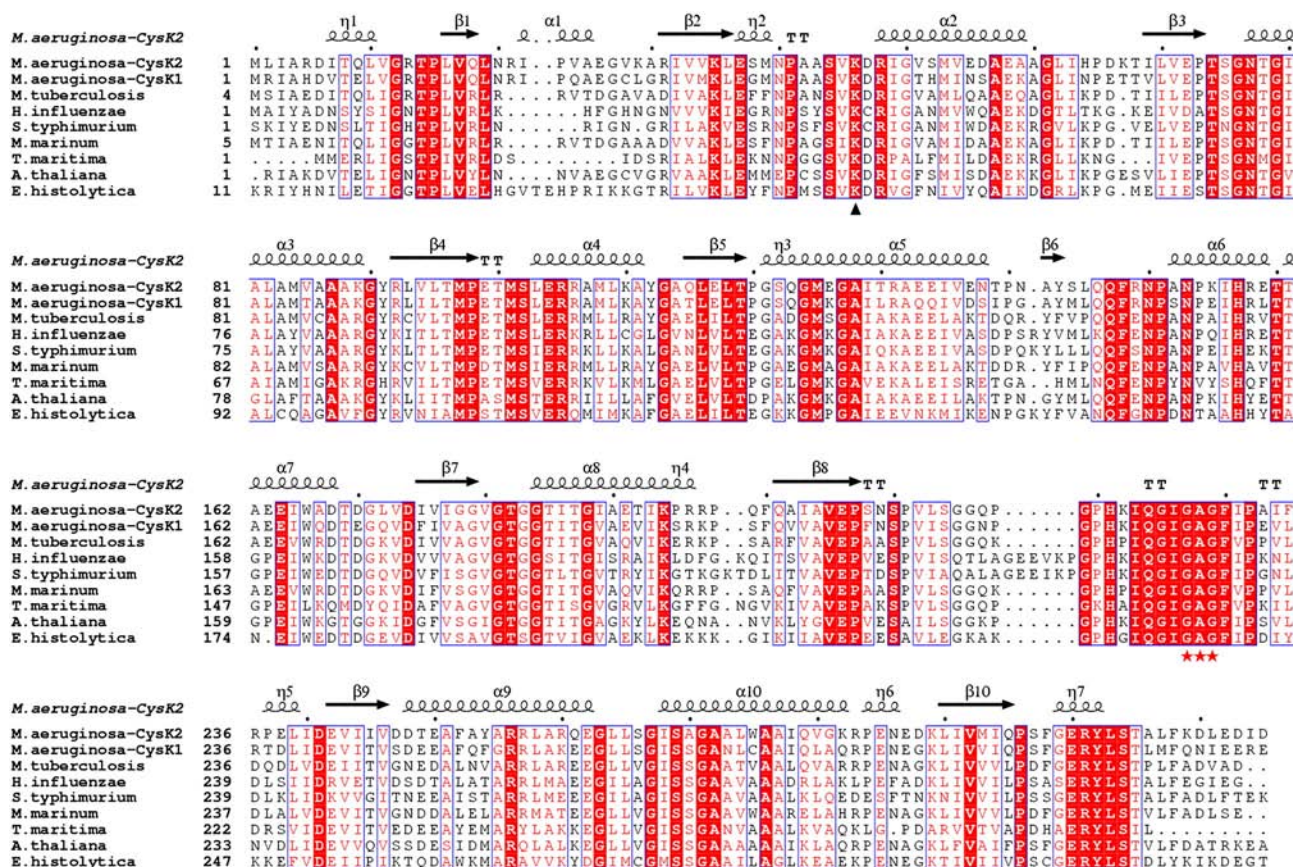


Fig. 1. Multiple-sequence alignment of CysK and homologs. The secondary structural elements of *M. aeruginosa* CysK2 were labeled on the top. The PLP-binding residue was labeled with black triangle and the shared “GAC” motif was marked with red asterisks. Colors are chosen according to rules of ESPript (<http://esprict.ibcp.fr/ESPript/ESPript/>): a blue frame represents a similarity across groups; a red character indicates similarity in a group; and a red box, white character demonstrates strict identity. All sequences were downloaded from the PDB database (<http://www.pdb.org/pdb/home/home.do>). The sequences are (PDB codes in parentheses) *Mycobacterium tuberculosis* OASS (2Q3D), *Haemophilus influenzae* OASS (1Y7L), *Salmonella typhimurium* OASS (1OAS), *Mycobacterium marinum* Atcc Baa-535 OASS (3RR2), *Thermotoga maritima* OASS (3FCA), *Arabidopsis thaliana* OASS (2ISQ), and *Entamoeba histolytica* OASS (2PQM).

conformational changes lead to a closed active site, which has been found in other complex structures of CysK [24–28].

3.3. The binding sites of PLP and cystine

At the active sites of both CysK1 and CysK2–cystine structures, the electron density map defined that PLP form a Schiff base with the Nε

atom of the conserved catalytic residue Lys46. The PLP molecule and its binding site undergo very slight conformational changes upon cystine binding, thus we took CysK2–cystine as an example to describe the PLP binding pattern. As shown in Fig. 2A, PLP is located in a cleft between the N- and C-terminal domains. The phosphate group of PLP interacts with the highly conserved Gly/Thr-rich loop (G¹⁸¹TGGT¹⁸⁵) and a water molecule Wat1 (Fig. 3A). The nitrogen atom of the pyridine

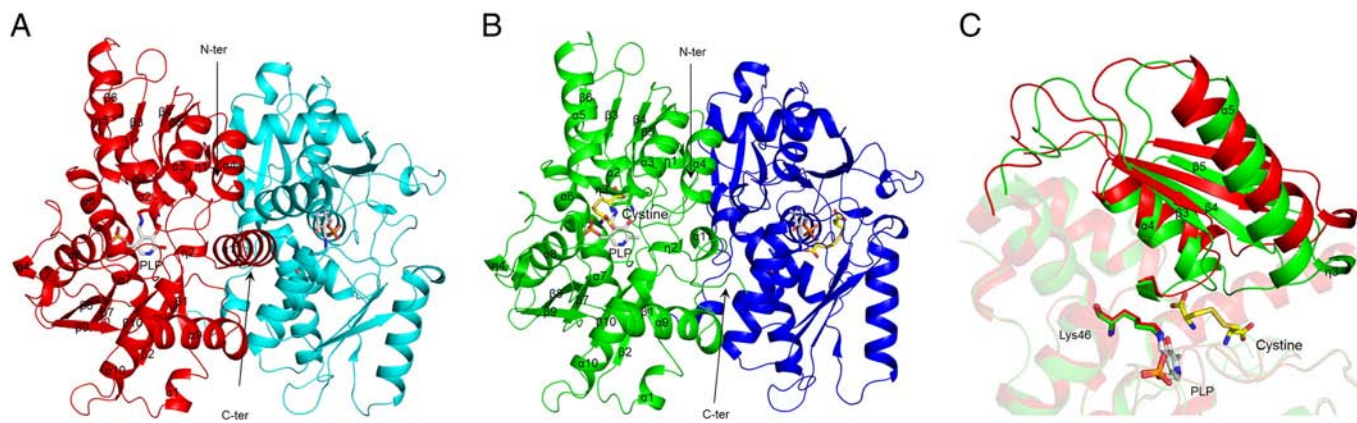


Fig. 2. Overall structures of CysK1 and CysK2–cystine. A) Cartoon representation of the CysK1 homodimer (red and cyan for each monomer, respectively). PLP molecules are shown as stick models and colored according to their atom type (C, gray; P, orange; N, blue; O, red). B) Cartoon representation of the CysK2–cystine homodimer (green and blue for each monomer, respectively). The secondary structural elements were labeled. Cystine molecules are shown as stick models and colored according to their atom type (C, yellow; N, blue; O, red; S, wheat). C) Superposition of CysK1 (red) and CysK2 (green) monomers showing the different position of the loop after cystine binding. PLP and cystine molecules are shown as stick models.

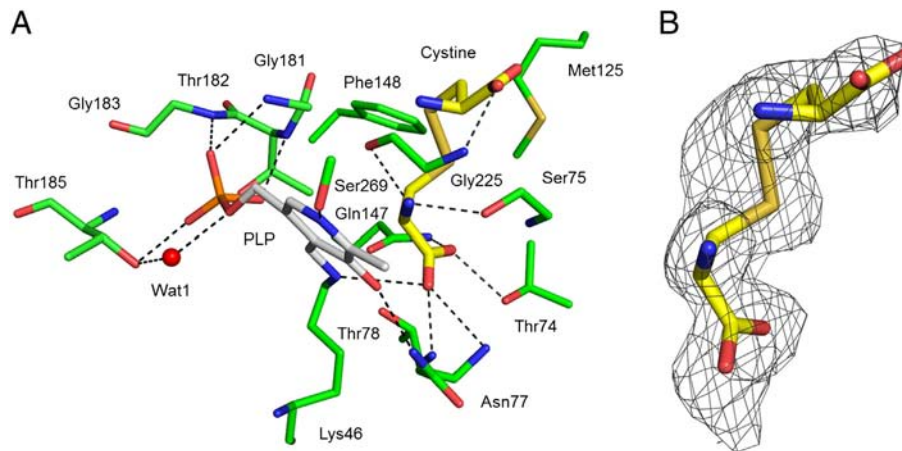


Fig. 3. The active site of CysK2–cysteine. A) The cystine and PLP binding site. The active-site residues were shown as sticks. B) Unbiased electron density map of cystine ($F_o - F_c$ map in gray at 1.5σ).

ring forms a hydrogen bond with the side chain of Ser269, which is located in the highly conserved helix $\alpha 10$. The hydroxyl group of PLP is stabilized via a hydrogen bond with the side chain of Asn77 in the highly conserved sequence stretch T⁷⁴SGNT⁷⁸.

As an initial attempt to get the complex structures of CysK1 and CysK2 with the product cysteine, we co-crystallized the proteins with 10 mM cysteine. However, we only found an extra electron density adjacent to the PLP molecule in the final model of CysK2, indicating

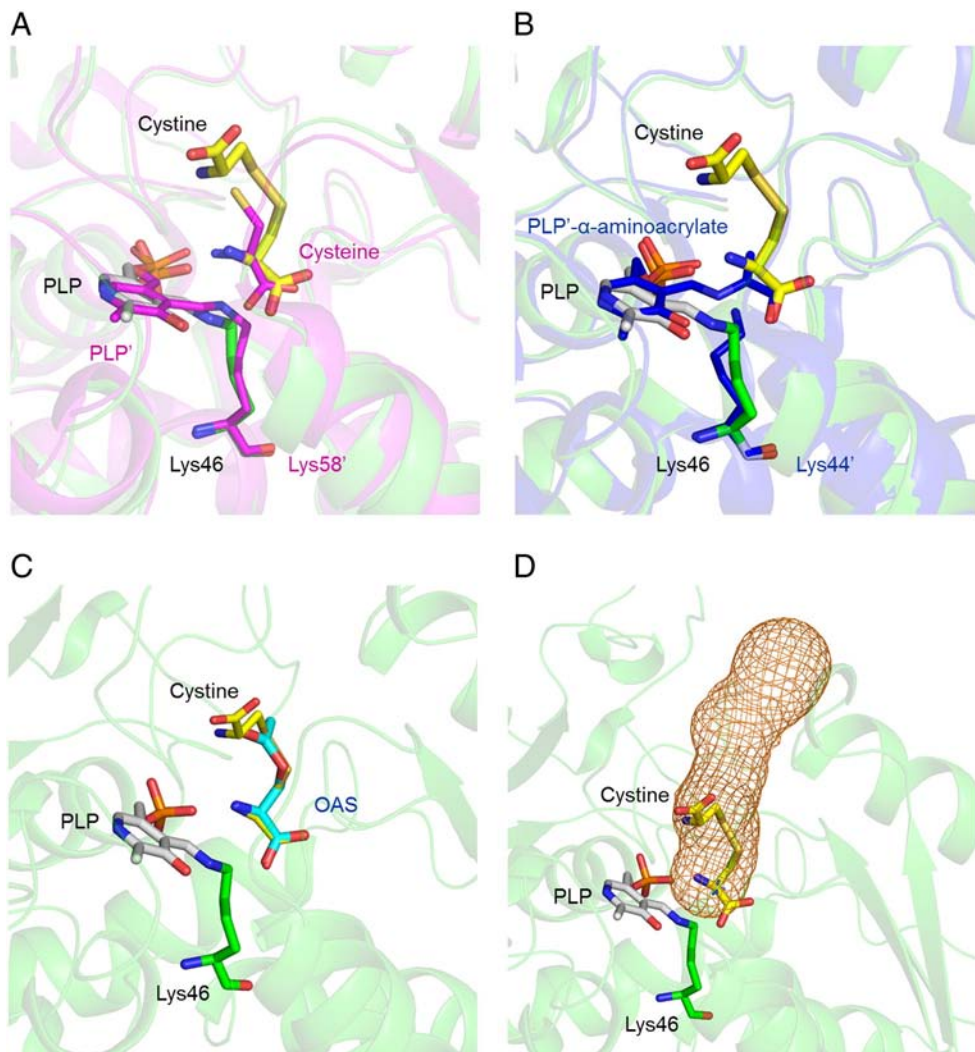


Fig. 4. Stereo representation of active-site comparison of CysK2 (green) with A) *Entamoeba histolytica* OASS (pink, PDB ID: 3BM5) and B) *Mycobacterium tuberculosis* CysK1 (blue, PDB ID: 2Q3B). C) A docking model of substrate OAS (cyan) bound to the active-site pocket of CysK2. D) A putative substrate-entrance or product-release tunnel calculated by the program CAVER denoted in brown mesh. PLP and cystine molecules are shown as stick models.

Table 2 K_i values of CysK1 and CysK2 towards OAS and cysteine, cystine.

	OAS (μM)	Cysteine (μM)	Cystine (μM)
CysK1	324 ± 71	1240 ± 236	239 ± 33
CysK2	142 ± 71	975 ± 258	186 ± 30

the presence of a small molecule. We first tried to fit the density with cysteine or other metabolites in the cysteine biosynthesis pathway, or reagents used during crystallization, but none of them matches. Considering the oxidation of cysteine during crystallization, we finally fit a molecule of cystine to the electron density map (Fig. 3B). The two cysteine moieties of cystine adopt opposite conformations, with the carboxyl groups pointing inward and outward, thus were termed Cys-in and Cys-out, respectively. The cystine is fixed in the active-site pocket of CysK2 through hydrogen bonds and hydrophobic interactions. The nitrogen atom of Cys-in is hydrogen-bonded by the side chain of Ser75 and the carbonyl oxygen of Gly225 (Fig. 3A). The two oxygen atoms of the carboxyl group of Cys-in are stabilized via three hydrogen bonds to the backbone amide groups of Asn77, Thr78, and N ϵ atom of Lys46, and two hydrogen bonds with the side chains of Gln147 and Thr74, respectively. One of the two carboxyl oxygen atoms of Cys-out makes a hydrogen bond with the main-chain nitrogen of Gly225. In addition, the disulfide bond of cystine is sandwiched by two hydrophobic residues Met125 and Phe148 on both sides (Fig. 3A).

3.4. The cystine occupies the substrate/product binding site of OASS

We superimposed the cystine-binding site of CysK2–cystine structure against those of the complex structures of OASS with the product cysteine and intermediates α -aminoacrylate, respectively [26,27]. The Cys-in of CysK2–cystine can be well superimposed to the cysteine of *E. histolytica* OASS (Fig. 4A). In addition, it could be well superimposed to the α -aminoacrylate moiety of PLP- α -aminoacrylate of *M. tuberculosis* CysK1 (Fig. 4B). Due to the absence of a complex structure with the substrate OAS, we constructed a docking model of CysK2–OAS using the software HADDOCK (<http://haddock.science.uu.nl/index.html>) [43,44]. The Cys-in of CysK2–cystine could be well superimposed to serine moiety of the docked OAS (Fig. 4C). These superposition results indicated that the Cys-in of CysK2 occupies the binding site for the substrate/product of OASS.

To compare their binding affinities, OAS, cysteine and cystine were titrated against CysK1 and CysK2, respectively. In fact, the affinities of cystine to CysK1 and CysK2 (239 ± 33 and 186 ± 30 μM) are comparable to those of OAS (324 ± 71 and 142 ± 71 μM) (Table 2). In contrast, the K_d values of cysteine to CysK1 and CysK2 are much higher (1240 ± 236 and 975 ± 258 μM) (Fig. S1). The low affinity of cysteine to CysK1/CysK2 is in agreement with the fact that product is ready for being released from the enzyme. The competitive affinity of cystine makes it a reasonable competitor to the substrate OAS.

Furthermore, we calculated a substrate-entrance or product-release tunnel of CysK2 using the program CAVER (<http://loschmidt.sci.muni.cz/caver/>). As shown in Fig. 4D, the substrate is proposed to approach the active site through a well-defined tunnel, which might be shared by the product to release. As seen in the CysK2–cystine structure, the tunnel is completely blocked by the cystine, which might function as a competitive inhibitor against the substrate of OASS. In consequence, we determined the inhibition constant (K_i) of cystine towards CysK1 and CysK2, and revealed a K_i value of 175 ± 27 and 155 ± 40 μM , respectively (Fig. 5). These K_i values are apparently comparable to the corresponding K_d values. These K_i values are also comparable to that of a C-terminal decapeptide fragment of *M. tuberculosis* SAT that can occupy the substrate binding pocket of OASS [26], and that of synthetic peptides mimicking a C-terminal of SAT inhibition of OASS-A from *Haemophilus influenzae* [17]. The physiological level of cysteine in bacteria is in the range from 0.1 to 0.2 mM as previously reported [45,46].

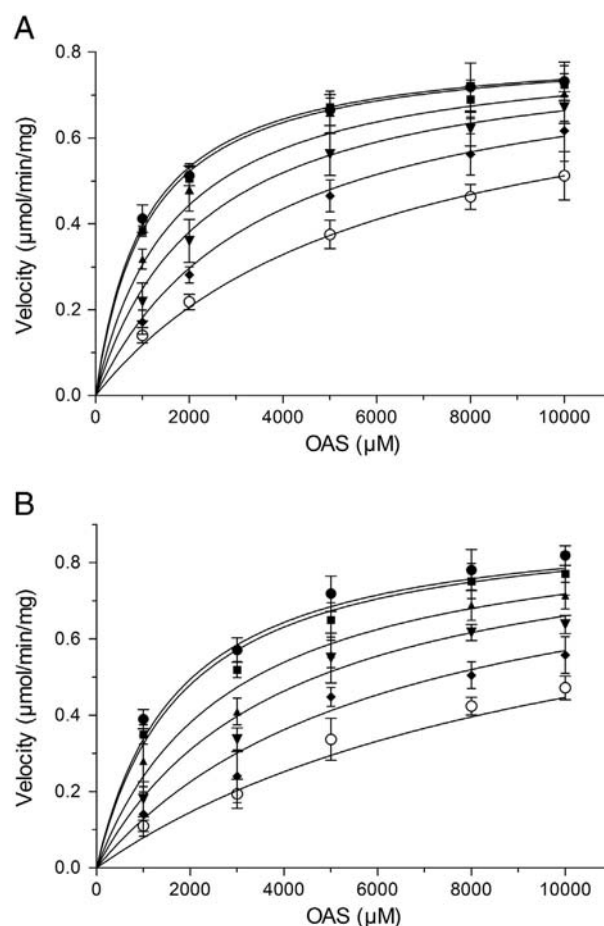


Fig. 5. Inhibition of CysK1 and CysK2 by cystine. Inhibition of cystine towards A) CysK1 and B) CysK2. The nonlinear curves were fitted to the data (average of measurements from three independent reactions) at cystine concentrations of 0 (\bullet), 10 (\blacksquare), 100 (\blacktriangle), 200 (\blacktriangledown), 400 (\blacklozenge), and 800 μM (\circ).

These K_i values at the hundred-micromolar level are comparable to the physiological concentration of cystine and cysteine. Thus we propose that cystine may effectively compete with the substrate OAS in vivo.

3.5. The redox-dependent auto-regulation of OASS

Given that the OASS could be inhibited by cystine, which is formed by the product cysteine upon oxidation, we further questioned if OASS is subject to the redox-dependent regulation. Firstly, we monitored the amount of synthesized cysteine as a function of time to detect the effect of redox on OASS (Fig. S2). With the addition of DTT, the production of cysteine reaches the maximum of 300 μM at 15 min. Meanwhile, in the oxidative reaction with addition of GSSG, the total amount of cysteine reaches the maximum of 200 μM at 20 min. These results suggest a negative feedback regulation of cysteine biosynthesis. Moreover, this concentration of cysteine is comparable to physiological level of cysteine at 0.1 to 0.2 mM in bacteria [46]. Then, we compared the enzymatic activities of CysK1 and CysK2 with and without the addition of GSSG and DTT, respectively. The activity of CysK1 or CysK2 with DTT is about 3–4 fold to that with GSSG (Table 3). The decrease of activity upon the addition GSSG is mostly due to the increase of K_m value towards OAS. In fact, the increase of GSSG-to-GSH ratio is along with the redox potential shifted to oxidation, resulting in the oxidation of cysteine to cystine. In turn, the cystine will compete with the same binding site of OAS, thus increasing the K_m value of OASS towards OAS.

Table 3
Kinetics parameters of CysK1 and CysK2 towards OAS.

	k_{cat} (s^{-1})	K_m (mM)	k_{cat}/K_m ($mM^{-1} s^{-1}$)
CysK1	136 ± 7	1.8 ± 0.3	76.5 ± 2.4
CysK1 + DTT	132 ± 3	1.0 ± 0.1	136 ± 2
CysK1 + GSSG	140 ± 3	3.5 ± 0.3	39.8 ± 1.2
CysK2	211 ± 7	2.3 ± 0.2	91.3 ± 0.3
CysK2 + DTT	232 ± 0	1.1 ± 0.2	219 ± 0
CysK2 + GSSG	231 ± 8	4.8 ± 0.5	48.1 ± 1.7

3.6. A putative feedback inhibition mechanism of cystine towards OASS

To check the evolutionary conservation of cystine-binding pattern, the sequences of OASSs from the model organisms of all three kingdoms were aligned (Fig. 6). The residues Thr74, Ser75, Asn77, Thr78, Gln147 and Gly225 which were involved in Cys-in binding are strictly conserved. Moreover, the two hydrophobic residues (Met125 and Phe148 in the case of CysK2) which sandwich the disulfide bond of cystine are strictly conserved. In addition, the loop containing Gly225, the main

chain nitrogen of which forms a hydrogen bond with Cys-out of cystine, is also conserved (Fig. 6). This suggested that the auto-inhibition of cystine might be a universal mechanism to all OASSs. Moreover, this negative feedback regulation provides a novel mechanism to the regulatory circuit of cysteine biosynthesis pathway.

Acknowledgements

We thank the assistance of the staff at Shanghai Synchrotron Radiation Facility. We are grateful to all the developers of CCP4 Suit, ESPrpt, MolProbit and PyMOL. This work was supported by the National Natural Science Foundation of China (Grant No. 31070652) and China Postdoctoral Science Foundation (2013M530297).

Appendix A. supplementary data

Supplementary data to this article can be found online at <http://dx.doi.org/10.1016/j.bbapap.2013.11.008>.

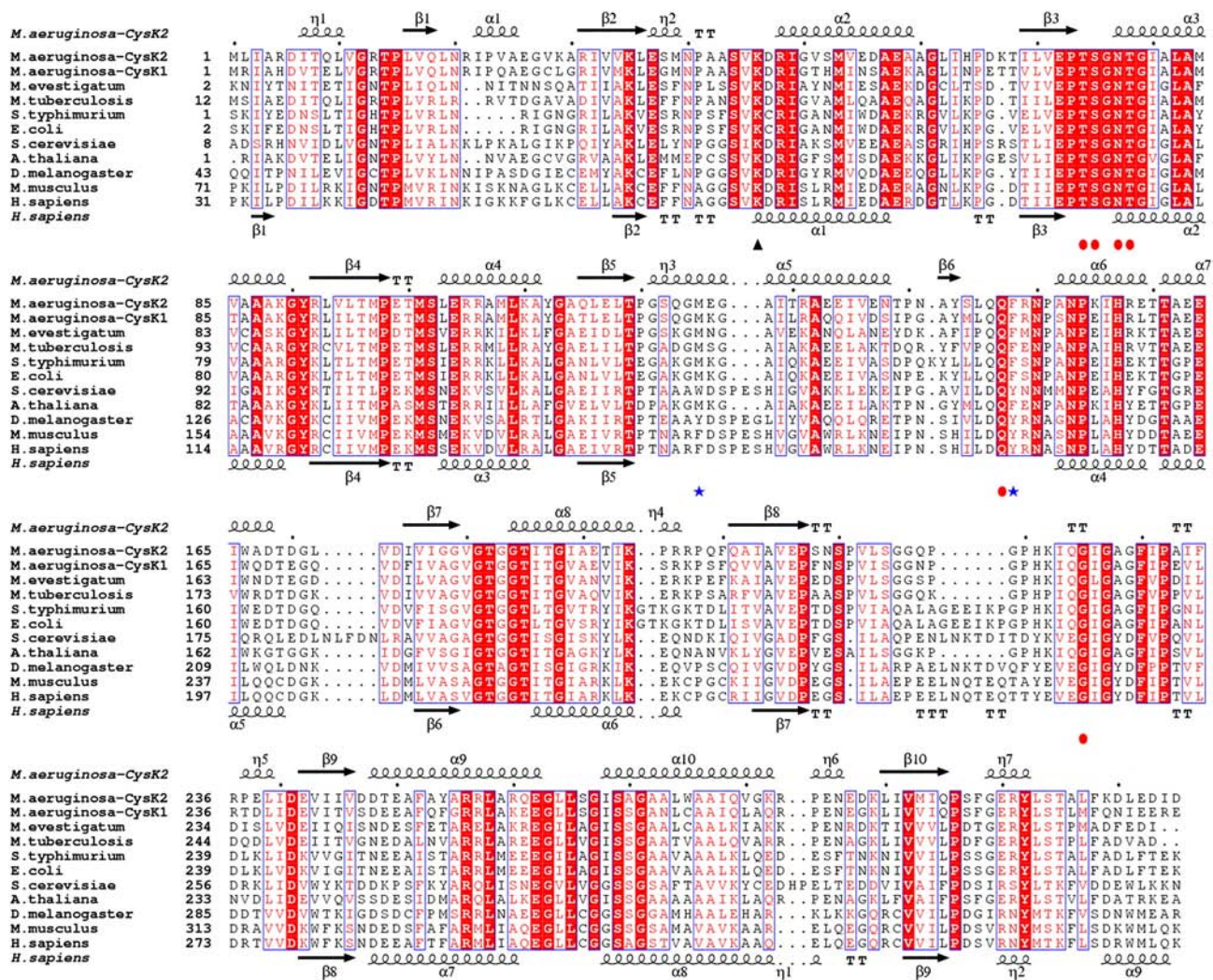


Fig. 6. Structure-based multiple-sequence alignment of CysK against other OASSs from the model organisms. The secondary structural elements of *Microcystis aeruginosa* CysK2 and *Homo sapiens* cystathionine-beta synthase were labeled on the top and bottom, respectively. The PLP-binding lysine was labeled with a black triangle, the Cys-in binding residues were marked with red dots and the residues interacting with disulfide bond in the middle of cystine were marked with blue asterisks. Colors are chosen according to rules of ESPrpt. All sequences were downloaded from the NCBI database (www.ncbi.nlm.nih.gov). The sequences are (NCBI accession numbers codes in parentheses) *Methanohalobium evestigatum* Z-7303 cysteine synthase A (YP_003727506.1), *Mycobacterium tuberculosis* CDC1551 cysteine synthase (NP_336875.1), *Salmonella typhimurium* cysteine synthase A (NP_456967.1), *Escherichia coli* cysteine synthase A (WP_000034411.1), *Saccharomyces cerevisiae* FostersB Cys4p (CGA58646.1), *Arabidopsis thaliana* O-acetylserine (thiol)lyase (OAS-TL) isoform A1 (NP_193224.1), *Drosophila melanogaster* cystathionine-beta Synthase (NP_608424.1), *Mus musculus* cystathionine-beta synthase (EDL40349.1), and *Homo sapiens* cystathionine-beta synthase (BAH11822.1).

References

- [1] P.F. Cook, C.H. Tai, C.C. Hwang, E.U. Woehl, M.F. Dunn, K.D. Schnackerz, Substitution of pyridoxal 5'-phosphate in the O-acetylserine sulfhydrylase from *Salmonella typhimurium* by cofactor analogs provides a test of the mechanism proposed for formation of the α -aminoacrylate intermediate, *J. Biol. Chem.* 271 (1996) 25842–25849.
- [2] W.M. Rabeh, P.F. Cook, Structure and mechanism of O-acetylserine sulfhydrylase, *J. Biol. Chem.* 279 (2004) 26803–26806.
- [3] C.H. Tai, P.F. Cook, Pyridoxal 5'-phosphate-dependent α , β -elimination reactions: mechanism of O-acetylserine sulfhydrylase, *Acc. Chem. Res.* 34 (2000) 49–59.
- [4] V.D. Rege, N.M. Kredich, C.H. Tai, W.E. Karsten, K.D. Schnackerz, P.F. Cook, A change in the internal aldimine lysine (K42) in O-acetylserine sulfhydrylase to alanine indicates its importance in transamination and as a general base catalyst, *Biochemistry* 35 (1996) 13485–13493.
- [5] K.D. Schnackerz, J.H. Ehrlich, W. Giesemann, T.A. Reed, Mechanism of action of D-serine dehydratase. Identification of a transient intermediate, *Biochemistry* 18 (1979) 3557–3563.
- [6] W.M. Rabeh, S.S. Alguindigues, P.F. Cook, Mechanism of the addition half of the O-acetylserine sulfhydrylase-A reaction, *Biochemistry* 44 (2005) 5541–5550.
- [7] C.H. Tai, S.R. Nalabolu, J.W. Simmons III, T.M. Jacobson, P.F. Cook, Acid-base chemical mechanism of O-acetylserine sulfhydrylases-A and -B from pH studies, *Biochemistry* 34 (1995) 12311–12322.
- [8] S. Kumaran, H. Yi, H.B. Krishnan, J.M. Jez, Assembly of the cysteine synthase complex and the regulatory role of protein–protein interactions, *J. Biol. Chem.* 284 (2009) 10268–10275.
- [9] E. Salsi, B. Campanini, S. Bettati, S. Raboni, S.L. Roderick, P.F. Cook, A. Mozzarelli, A two-step process controls the formation of the bienzyme cysteine synthase complex, *J. Biol. Chem.* 285 (2010) 12813–12822.
- [10] L.R. Olsen, B. Huang, M.W. Vetting, S.L. Roderick, Structure of serine acetyltransferase in complexes with CoA and its cysteine feedback inhibitor, *Biochemistry* 43 (2004) 6013–6019.
- [11] A. Mozzarelli, S. Bettati, B. Campanini, E. Salsi, S. Raboni, R. Singh, F. Spyrakis, V.P. Kumar, P.F. Cook, The multifaceted pyridoxal 5'-phosphate-dependent O-acetylserine sulfhydrylase, *Biochim. Biophys. Acta* 1814 (2011) 1497–1510.
- [12] Ö. Poyraz, V.U. Jeankumar, S. Saxena, R. Schnell, M. Haraldsson, P. Yogeewari, D. Sriram, G. Schneider, Structure-guided design of novel thiazolidine inhibitors of O-acetylserine sulfhydrylase from *Mycobacterium tuberculosis*, *J. Med. Chem.* 56 (2013) 6457–6466.
- [13] H. Tian, R. Guan, E. Salsi, B. Campanini, S. Bettati, V.P. Kumar, W.E. Karsten, A. Mozzarelli, P.F. Cook, Identification of the structural determinants for the stability of substrate and aminoacrylate external Schiff bases in O-acetylserine sulfhydrylase-A, *Biochemistry* 49 (2010) 6093–6103.
- [14] S. Kumaran, J.M. Jez, Thermodynamics of the interaction between O-acetylserine sulfhydrylase and the C-terminus of serine acetyltransferase, *Biochemistry* 46 (2007) 5586–5594.
- [15] W.-S. Kim, D. Chronis, M. Juergens, A.C. Schroeder, S.W. Hyun, J.M. Jez, H.B. Krishnan, Transgenic soybean plants overexpressing O-acetylserine sulfhydrylase accumulate enhanced levels of cysteine and Bowman–Birk protease inhibitor in seeds, *Planta* 235 (2012) 13–23.
- [16] A. Chattopadhyay, M. Meier, S. Ivaninskii, P. Burkhard, F. Speroni, B. Campanini, S. Bettati, A. Mozzarelli, W.M. Rabeh, L. Li, Structure, mechanism, and conformational dynamics of O-acetylserine sulfhydrylase from *Salmonella typhimurium*: comparison of A and B isozymes, *Biochemistry* 46 (2007) 8315–8330.
- [17] E. Salsi, A.S. Bayden, F. Spyrakis, A. Amadasi, B. Campanini, S. Bettati, T. Dodatko, P. Cozzini, G.E. Kellogg, P.F. Cook, S.L. Roderick, A. Mozzarelli, Design of O-acetylserine sulfhydrylase inhibitors by mimicking nature, *J. Med. Chem.* 53 (2009) 345–356.
- [18] R. Schnell, G. Schneider, Structural enzymology of sulphur metabolism in *Mycobacterium tuberculosis*, *Biochem. Biophys. Res. Commun.* 396 (2010) 33–38.
- [19] T. Nakamura, Y. Kon, H. Iwahashi, Y. Eguchi, Evidence that thiosulfate assimilation by *Salmonella typhimurium* is catalyzed by cysteine synthase B, *J. Bacteriol.* 156 (1983) 656–662.
- [20] T. Nakamura, H. Iwahashi, Y. Eguchi, Enzymatic proof for the identity of the S-sulfocysteine synthase and cysteine synthase B of *Salmonella typhimurium*, *J. Bacteriol.* 158 (1984) 1122–1127.
- [21] M.T. Claus, G.E. Zocher, T.H. Maier, G.E. Schulz, Structure of the O-acetylserine sulfhydrylase isoenzyme CysM from *Escherichia coli*, *Biochemistry* 44 (2005) 8620–8626.
- [22] G. Schneider, H. Käck, Y. Lindqvist, The manifold of vitamin B6 dependent enzymes, *Structure* 8 (2000) R1–R6.
- [23] N.V. Grishin, M.A. Phillips, E.J. Goldsmith, Modeling of the spatial structure of eukaryotic ornithine decarboxylases, *Protein Sci.* 4 (1995) 1291–1304.
- [24] P. Burkhard, C.H. Tai, C.M. Ristroph, P.F. Cook, J.N. Jansonius, Ligand binding induces a large conformational change in O-acetylserine sulfhydrylase from *Salmonella typhimurium*, *J. Mol. Biol.* 291 (1999) 941–953.
- [25] E.R. Bonner, R.E. Cahoon, S.M. Knapke, J.M. Jez, Molecular basis of cysteine biosynthesis in plants structural and functional analysis of O-acetylserine sulfhydrylase from *Arabidopsis thaliana*, *J. Biol. Chem.* 280 (2005) 38803–38813.
- [26] R. Schnell, W. Oehlmann, M. Singh, G. Schneider, Structural insights into catalysis and inhibition of O-acetylserine sulfhydrylase from *Mycobacterium tuberculosis*, *J. Biol. Chem.* 282 (2007) 23473–23481.
- [27] K. Chinthalapudi, M. Kumar, S. Kumar, S. Jain, N. Alam, S. Gourinath, Crystal structure of native O-acetylserine sulfhydrylase from *Entamoeba histolytica* and its complex with cysteine: structural evidence for cysteine binding and lack of interactions with serine acetyl transferase, *Proteins Struct. Funct. Genet.* 72 (2008) 1222–1232.
- [28] H. Yi, M. Juergens, J.M. Jez, Structure of soybean β -cyanoalanine synthase and the molecular basis for cyanide detoxification in plants, *Plant Cell* 24 (2012) 2696–2706.
- [29] B. Huang, M.W. Vetting, S.L. Roderick, The active site of O-acetylserine sulfhydrylase is the anchor point for bienzyme complex formation with serine acetyltransferase, *J. Bacteriol.* 187 (2005) 3201–3205.
- [30] H.S. Lee, G. Spraggon, P.G. Schultz, F. Wang, Genetic incorporation of a metalion chelating amino acid into proteins as a biophysical probe, *J. Am. Chem. Soc.* 131 (2009) 2481–2483.
- [31] Z. Otwinowski, M. Minor, Processing of X-ray diffraction data, *Methods Enzymol.* 276 (1997) 307–326.
- [32] A. Vagin, A. Teplyakov, Molecular replacement with MOLREP, *Acta Crystallogr. D Biol. Crystallogr.* 66 (2010) 22–25.
- [33] G.N. Murshudov, A.A. Vagin, E.J. Dodson, Refinement of macromolecular structures by the maximum-likelihood method, *Acta Crystallogr. D Biol. Crystallogr.* 53 (1997) 240–255.
- [34] N. Collaborative Computational Project, The CCP4 suite: programs for protein crystallography, *Acta Crystallogr. D Biol. Crystallogr.* 50 (1994) 760–763.
- [35] P. Emsley, K. Cowtan, Coot: model-building tools for molecular graphics, *Acta Crystallogr. D Biol. Crystallogr.* 60 (2004) 2126–2132.
- [36] V.B. Chen, W.B. Arendall, J.J. Headd, D.A. Keedy, R.M. Immormino, G.J. Kapral, L.W. Murray, J.S. Richardson, D.C. Richardson, MolProbity: all-atom structure validation for macromolecular crystallography, *Acta Crystallogr. D Biol. Crystallogr.* 66 (2009) 12–21.
- [37] R.A. Laskowski, M.W. MacArthur, D.S. Moss, J.M. Thornton, PROCHECK: a program to check the stereochemical quality of protein structures, *J. Appl. Crystallogr.* 26 (1993) 283–291.
- [38] W.L. DeLano, The PyMOL Molecular Graphics System, 2002.
- [39] M.K. Gaitonde, A spectrophotometric method for the direct determination of cysteine in the presence of other naturally occurring amino acids, *Biochem. J.* 104 (1967) 627–633.
- [40] I. Nagpal, I. Raj, N. Subbarao, S. Gourinath, Virtual screening, identification and in vitro testing of novel inhibitors of O-acetyl-L-serine sulfhydrylase of *Entamoeba histolytica*, *PLoS ONE* 7 (2012) e30305.
- [41] A. Cornish-Bowden, Fundamentals of Enzyme Kinetics, Portland Press Ltd., London, UK, 2004.
- [42] W.E. Karsten, P.F. Cook, Detection of intermediates in reactions catalyzed by PLP-dependent enzymes: O-acetylserine sulfhydrylase and serine-glyoxalate aminotransferase, *Methods Enzymol.* 354 (2002) 223–237.
- [43] C. Dominguez, R. Boelens, A.M. Bonvin, HADDOCK: a protein–protein docking approach based on biochemical or biophysical information, *J. Am. Chem. Soc.* 125 (2003) 1731–1737.
- [44] S.J. De Vries, A.D. Van Dijk, M. Krzeminski, M. Van Dijk, A. Thureau, V. Hsu, T. Wassenaar, A.M. Bonvin, HADDOCK versus HADDOCK: new features and performance of HADDOCK2.0 on the CAPRI targets, *Proteins* 69 (2007) 726–733.
- [45] M. Noji, K. Inoue, N. Kimura, A. Gouda, K. Saito, Isoform-dependent differences in feedback regulation and subcellular localization of serine acetyltransferase involved in cysteine biosynthesis from *Arabidopsis thaliana*, *J. Biol. Chem.* 273 (1998) 32739–32745.
- [46] S. Park, J.A. Imlay, High levels of intracellular cysteine promote oxidative DNA damage by driving the Fenton reaction, *J. Bacteriol.* 185 (2003) 1942–1950.